Bull Mater Sci (2020)43:199
https://doi.org/10.1007/s12034-020-02168-6

Diffuse spectra model of photoluminescence in carbon quantum dots

S E KUMEKOV[1], N K SAITOVA[1] and K S MARTIROSYAN[2,*]
[1]Satbayev University, 050013 Almaty, Kazakhstan
[2]Department of Physics and Astronomy, University of Texas at Rio Grande Valley, Brownsville, TX 78520, USA
*Author for correspondence (karen.martirosyan@utrgv.edu)

MS received 20 March 2020; accepted 18 May 2020

Abstract. The attractive aspect of excitation related to fluorescence nature in carbon quantum dots (CQD) has guided to several assumptions correlated with clusters size distribution, shapes as well as presence of different emissive states. In this study, a dimer–excimer model of photoluminescence (PL) in CQD describing discrete multiple electronic states for the excitation-dependent emission is described. The functional dependence of the characteristic width of the diffuse spectra of PL on the size of a quantum dots are calculated. The effective width of PL spectrum can be tuned from 0.1 to 1 eV.

Keywords. Carbon; quantum dots; excimer; photoluminescence spectrum.

1. Introduction

The interesting features of the photoluminescence (PL) in carbon quantum dots (CQD) have been revealed recently [1–6]. Numerous papers discuss different nature of PL mechanism in CQD [4–7]: quantum size effect, defects and surface states, surface groups, surface passivation, fluorophores and various degrees of π-electron coupling, recombination of electron–hole pairs localized in the interior of small sp^2 clusters, embedded in sp^3 matrix. The carbon dots have an excellent luminescence property and water solubility, as well as excellent biocompatibility [7]. The technologies of the preparation of CQD are based on different materials and methods, which can be divided into three groups: graphene-like clusters, graphitized clusters and polymeric CQD. All the objects share one common structural property: presence of carbon hexagons—nuclei of the benzene ring.

The structural feature of the above objects can lead to the formation of sandwich structures [8–10], representing physical dimers of carbon hexagons—aromatic rings or their combination. The term 'dimer' implies a physical dimer consisting of two monomers [11]. Dimers can be of different types of geometries. Dimers with the parallel arrangement of monomers have sandwich structure. It is about these dimers that are discussed in this article. In such dimers, monomers are considered as flat graphene-like clusters of different sizes, depending on the number of hexagons forming the cluster.

In this study, such a representation of the structure of CQD allows to develop a dimer–excimer model of radiative processes and to calculate the spectral characteristics of PL spectra in CQD. A diffuse luminescence model based on radiative transitions from a discrete level to continuum [12,13] is used to calculate the spectral characteristics. The excimer nature of PL in CQD, in particular based on graphite, can be assumed for the following reason: given the size of a CQD within several nanometres, the electronic spectrum of graphite would be subject essentially to size quantization (at the effective electron mass of $m^* = 0.4m_0$ [14]).

The energy interval between the neighbouring size quantization levels significantly exceeds the thermal energy of electrons in the conduction band. This circumstance suggests the dominant role of molecular terms in the formation of PL spectra. It is appropriate to notice the analogy of graphite with crystals of pyrene and fluorine [9,10]. The distance between the adjacent graphene-like layers in graphite bound by van der Waals forces is 3.37 Å. For pyrene crystals, semi-empirical calculations yield the average distance between unexcited monomers in dimer to be 3.53 Å, while that in excimer to be 3.37 Å [8].

2. The governing model

The formation of excimers in gases, liquid solutions and crystals can occur according to different schemes [8]. In gases and fairly diluted solutions of the excimer-forming monomer, excimer could be formed through optical excitation of a monomer with its subsequent approach to a neighbouring monomer (remaining in the ground state) closely enough for a stable excimer state to be established at $R = R_e$ (figure 1). In that case, the absorption spectra of light by the monomer and the luminescence spectra of the excimer are located in significantly different spectral regions.

Published online: 12 August 2020

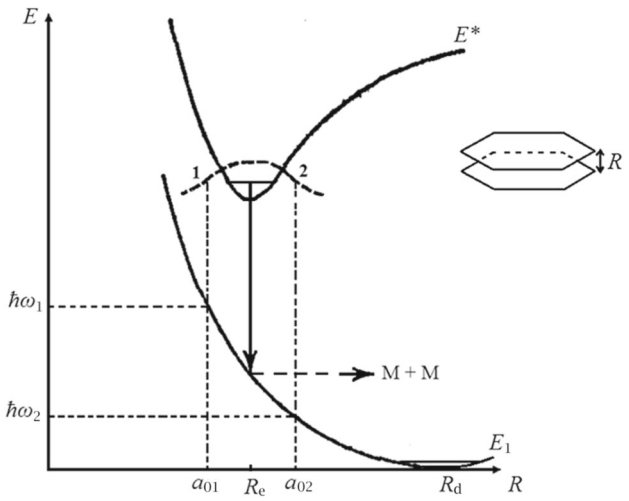

Figure 1. The origin of the diffuse emission spectrum of the excimer. E_1 and E^* are electronic terms of the ground and excited states of an excimer. 1 and 2 schematically illustrate the vicinity of the classical points of vibration of the zero level of the harmonic oscillator from which radiative optical transitions are possible. The bell-shaped curve illustrates the probability for the state of the excimer at the zero-vibrational level. The inset demonstrates geometrical structure of the dimer.

In crystals, regular elements of the crystal structure, such as monomers located in parallel ('imprinted' dimers), could become pre-dimer sites [8,11]. For example, in pyrene crystals, the interaction of pairs of molecules manifests itself even at the room temperature. As a result, a new component emerges in the absorption spectra of the pyrene crystal, offset by 20 nm towards the long-wave region relative to the molecular absorption band [15]. One may assume that a similar pattern could be observed in CQD. This is evidenced by a significant overlap of the absorption, PL and excitation spectra in these objects [5,6].

Pre-dimer sites in CQD can be considered as physical dimers in a regular graphitized structure. The physical dimer in CQD is represented as a sandwich structure consisting of plane-parallel monomers—graphene-like clusters. The geometry of the sandwich structures determines both the features of the experimental characteristics of PL and the theoretical consideration of CQD. The smallest cluster is a sandwich comprised by two parallel hexagonal carbon skeletons of benzene rings. In the monomer plane, carbon atoms are hybridized by the sp^2 bond. On the periphery of such a monomer, free carbon bonds can be compensated by H, N, O functional groups [1–3].

The CQD dimers and monomers are bound in the direction perpendicular to the monomer plane by weak long-range van der Waals forces, resembling the structure of graphite [13]. It is the van der Waals forces that balance the repulsive forces of exchange and Coulomb interactions between the graphene-like layers leading to a stable ground state E_1 of the dimer with a slight potential barrier at a separation $R = R_d$ between the monomers as presented in figure 1.

When describing an electron–nuclear system in terms of the adiabatic approximation, potential energies of the ground and excited electron states are graphically represented on the configuration diagram as functions of the inter nuclear or intermolecular separation [8–10]. Figure 1 shows the terms of the ground E_1 and excited states E^* of the dimer–excimer complex as a function of the distance R between the monomers [10]. The ground state E_1 in a crystal is featured by a repulsion at $R < R_d$ and a stable equilibrium at $R = R_d$.

Owing to the induced Coulomb interaction, the excited state of a dimer representing the excimer state corresponds to a stable state [8,11], but at distances between the monomers R_e smaller than in the stable ground state of the dimer R_d ($R_e < R_d$). The Hamiltonian, H, of the physical dimer can be written [10] as:

$$H = H_1 + H_2 + V_{12}, \tag{1}$$

where H_1 and H_2 are the Hamiltonians of the respective individual monomers, and $V_{12}(R)$ is the interaction energy between the monomers, depending on the distance of separation, R. In general, $V_{12}(R)$ is comprised by the exchange, V_{exc}, Coulomb, V_C, and van-der-Waals, V_{VW}, interactions.

The forces of exchange interaction are short-range and repulsive. The van der Waals interaction is long-range and attractive. The sign of the Coulomb interaction differs for the ground and the excited states of the dimer [11]. In the first case, the Coulomb force would be repulsive, while in the second case, it would be attractive. For this reason, the steady state of the excimer is reached at $R_e < R_d$ (figure 1).

Denoting the respective eigenvalues of the Hamiltonian equation (1) for dimer and excimer states as E_1 and E^*, we can write the steady-state equations as shown:

$$\frac{dE_1}{dR} = 0 \quad \text{at} \quad R = R_d, \quad \frac{dE^*}{dR} = 0 \quad \text{at} \quad R = R_e. \tag{2}$$

In accordance with equation (2), the depth of the potential well at $R = R_d$ determines the binding energy of the dimer and can be measured as the dissociation energy of the dimer in spectroscopic studies. The potential well depth at $R = R_e$ can be estimated from the long-wave edge of the excimer emission band. This property of radiative processes during the transitions from a discrete state to a continuous state of the spectrum was noted in the study by Spol'ski [12]. In figure 1, vertical arrows indicate optical transitions occurring when light is emitted from term E^* at $R = R_e$. The dashed arrow denotes the dissociation of a dimer into $M + M$ monomers in the ground state E_1.

3. Spectral characteristics of dimer–excimer systems

The main feature of dimer–excimer systems is the possibility of a photo-dissociation transition according to the scheme

$$E^* \rightarrow M + M + \hbar\omega. \tag{3}$$

In this process, the excimer transits to the ground state of the dimer E_1, which is repulsive at distances $R < R_d$ between the monomers. The dissociation results in a decay of the excimer into unexcited monomers M during the separation expansion time of about 1–10 ps. This photodissociation of the excimer, which takes place during the transition from the bound state E^* to the continuum state E_1, leads to the formation of a wide and structureless luminescence band (figure 1) [12,13]. The diffuse, wide and structureless emission bands are characteristic of radiative transitions from a discrete level to a continuum level. Such radiative transitions are categorized as fluorescent luminescence due to the decay nature of the final state [12]. Figure 1 represents the origin of the diffuse, wide and structureless luminescence band. The width of the spectrum depends on the slope of the potential energy curve of the electronic term E_1 and the distance between the backtracking points at the vibrational level of the E^* curve. From the states corresponding to the energy level with a quantum number v between the classical turning points a_{v1} and a_{v2}, optical transitions to the ground state E_1 can be performed in accordance with the adiabatic approximation. For example, the probability of finding the excimer at the zero level is shown schematically with a bell-shaped curve. To calculate the possible emission spectrum, the distance between the return points at the vibrational level of the excimer E^* is projected vertically in accordance with the Frank–Condon principle onto the E_1 curve and the intersection points are parallelly transferred to the energy scale. The projections of points on the energy scale are denoted as $\hbar\omega_1$ and $\hbar\omega_2$. The energy interval between $\hbar\omega_1$ and $\hbar\omega_2$ corresponds to the characteristic effective width of the spectrum Δ. The effective width in PL spectra Δ was calculated according to the following expression:

$$\Delta = \hbar\omega_1 - \hbar\omega_2 = (a_{v1} - a_{v2})\frac{dE_1}{dR}. \quad (4)$$

Considering the bottom of the excimer well near $R = R_e$ in a parabolic approximation, it is possible to estimate the spectral width for a structure with known parameters of a harmonic oscillator.

In the harmonic approximation, we can write the amplitude of monomer oscillations in the form

$$a_v = \left[\frac{\hbar(v+1/2)}{(k\mu)^{1/2}}\right]^{1/2} \quad (5)$$

where μ is the reduced mass of the monomer, k the coefficient of elasticity.

The calculation of the dependences of the effective width of the spectrum on the size of the object can be carried out for two simple cases (see figure 2): (1) the linear sandwich cluster of benzene rings of length L; (2) the cluster of sandwich benzene rings in the form of a disk with a diameter D.

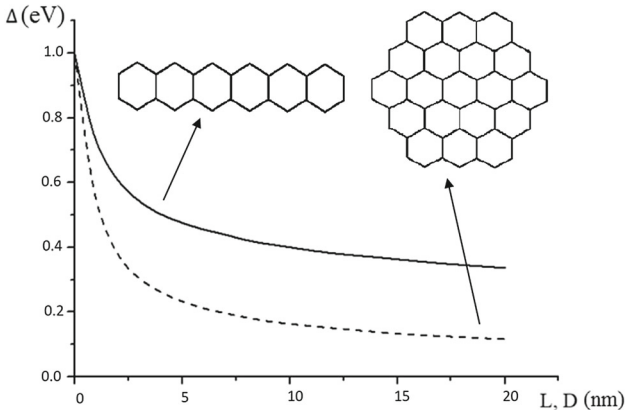

Figure 2. Dependence of the effective width of the PL spectrum Δ on the size of the quantum dot L, D. The solid curve is Δ_L and the dotted curve is Δ_D. Two types of dimers: Δ_L is the linear sandwich cluster of benzene rings of length L; and Δ_D is the cluster of sandwich benzene rings in the form of a disk with a diameter D. Cross size d_{C6} of the benzene ring is 0.28 nm.

The molar mass of the benzene ring μ_{C6} is 72 a.m.u., and its cross size d_{C6} is 0.28 nm [15,16]. Then from equation (5) follow the equations for the amplitudes of zero oscillations of monomers in a linear cluster a_{0L} and for a disk a_{0D}:

$$a_{0L} = \left[\frac{\hbar}{(2k\mu_{C6})^{1/2}}\right]^{1/2}\left(\frac{d_{C6}}{L}\right)^{1/4},$$

$$a_{0D} = \left[\frac{\hbar}{(2k\mu_{C6})^{1/2}}\right]^{1/2}\left(\frac{d_{C6}}{D}\right)^{1/2}.$$

The substitution of numerical parameters gives:

$$a_{0L}\ (\text{nm}) = 2.86 \cdot 10^{-3} L^{-1/4}, \quad (6)$$

$$a_{0D}\ (\text{nm}) = 2.08 \cdot 10^{-3} D^{-1/2}. \quad (7)$$

To calculate Δ by equation (4), it is necessary to find the curvature of the E_1 term. Electronic transitions to E_1 term in the configuration diagram (figure 1) occur in the vicinity of the point $R = R_e$. Therefore, it suffices to find the curvature of the term E_1 for $R = R_e$. To do this, we use the approximation of E_1 term by the pair Morse potential [17]. Then you can get:

$$\left(\frac{dE_1}{dR}\right)_{R=R_e} = -2\alpha E_d\{\exp[-2\alpha(R_e - R_d) - \exp[-\alpha(R_e - R_d)]]\}. \quad (8)$$

Here, α is a constant characterizing the width at $R = R_d$, E_d the dissociation energy of the ground state of the dimer, R_e and R_d are the coordinates of the steady state of the excimer and dimer, respectively (figure 1).

Substituting equations (6–8) into equation (4) and using the numerical values of the parameters $\alpha = 133.7\ \text{nm}^{-1}$,

$E_d = 0.05$ eV, $(R_e - R_d) = -0.01$ nm and $\left(\frac{dE_1}{dR}\right)_{R=R_e} = 124.3\ \text{eV nm}^{-1}$, we defined the equations for calculating the width of PL spectrum for two cases:

$$\Delta_L\ (\text{eV}) = 0.711L^{-1/4}, \tag{9}$$

$$\Delta_D\ (\text{eV}) = 0.517D^{-1/2}. \tag{10}$$

Figure 2 shows the dependences of the effective width of the PL spectrum for both cases including Δ_L (L) and Δ_D (D). The width of the PL spectrum with decreasing size reaches the values of the order of 1 eV, which is in qualitative agreement with the experimental results [1–3]. The dependences converge to the same value of the width of the spectrum with the values of L and D equal to the minimum cross size of the sandwich 0.28 nm.

The photo-dissociation cross-section of the excimer in the CQD for the adiabatic approximation is [13]

$$\sigma_{PD} = \frac{\pi^2 c^2 \hbar^3}{(\hbar\omega)^2 \Delta \tau_{sp}}, \tag{11}$$

here c is the speed of light, $\hbar\omega$ the radiation quantum energy, Δ the effective width of the emission band, τ_{sp} the lifetime of the excited state with respect to spontaneous transitions. In equation (11), it is essential to keep in mind the dependence of the effective width of the PL band on the size of the CQD according to equations (9 and 10).

PL can be characterized by various parameters such as the energy of the exciting photon with respect to the emission. The PL quantum yield is an important measure of luminescent materials. In this model, we consider that the repulsive ground state of the dimer–excimer complex E_1 is unstable with short-lived. Therefore, there is essentially always a population inversion between the excited singlet-state E^* and the ground state E_1. Such condition determines the high probability of fluorescent radiation transitions. The radiative transitions will be more competitive with respect to nonradiative transitions and provide the high quantum yield fluorescence [18]. In the study by Lin *et al* [19], the PL quantum yield of CQD was measured and the produced carbon dots exhibited a high-fluorescence quantum yield up to 85%.

4. Conclusions

In summary, we reported a dimer–excimer model of PL in CQD describing discrete multiple electronic states for the excitation-dependent emission. The characteristic effective width of the spectra of PL of CQD is calculated and shown that the effective width depends on shape and size of CQDs. The effective width of the PL spectrum with decreasing size reaches values of the order of 1 eV, which is in qualitative agreement with the reported experimental results.

Acknowledgements

SEK and NKS sincerely acknowledge the financial support by Grant No. 05132875 of the Ministry of Education and Science of the Republic of Kazakhstan.

References

[1] Tang L, Ji R, Cao X, Lin J, Jiang H, Li X *et al* 2012 *ACS Nano* **6** 5102
[2] Peng J, Gao W, Gupta B K, Liu Z, Romero-Aburto R, Ge L *et al* 2012 *Nano Lett.* **12** 844
[3] Sk M A, Ananthanarayanan A, Huang L, Lim K H and Chen P 2014 *J. Mater. Chem.* **2** 6954
[4] Lee H L, Woon K L, Tan S, Wong W S, Ariffin A, Chanlek N *et al* 2019 *Carbon Lett.* **29** 255
[5] Wang Y and Hu A 2014 *J. Mater. Chem.* **2** 6921
[6] Li F, Liu C, Yang J, Wang Z, Liu W and Tian F 2014 *RSC Adv.* **4** 3201
[7] Sharma A, Gadly T, Gupta A, Ballal A, Ghosh S K and Kumbhakar M 2016 *J. Phys. Chem. Lett.* **7** 3695
[8] Guillet J 1987 *Polymer photophysics and photochemistry* (Cambridge: Cambridge University Press) p 414
[9] Birks J B and Kazzaz A A 1968 *Proc. R. Soc. Lond. A* **304** 291
[10] Saigusa H and Lim E C 1991 *J. Phys. Chem.* **95** 2364
[11] Pope M and Swenberg C 1999 *Electronic processes in organic crystals and polymers*, 2nd edn (New York: Oxford University Press) p 1328
[12] Spol'ski E V 1933 *UFN* **8** 325
[13] Rhodes C K 1984 *Excimer lasers* (Heidelberg: Springer-Verlag) p 271
[14] Mc Clure J W 1964 *IBM J.* **8** 255
[15] Fischer D, Haukdorf G and Kloppfer W 1973 *Naturforch Z.* **A28** 973
[16] Glinka N and Sobolev D 1981 *General chemistry*, 7th edn (New York: M.E. Sharpe) p 694
[17] Kaplan I G 2003 in *Handbook of molecular physics and quantum chemistry* (Chichester: Wiley) p 207
[18] Berlman I 1971 *Handbook of fluorescence spectra of aromatic molecules* (New York: Academic Press) p 472
[19] Lin H, Huang J and Ding L 2019 *J. Nanomater.* Article ID 5037243, https://doi.org/10.1155/2019/5037243